



Geophysical Research Letters

RESEARCH LETTER

10.1029/2022GL097751

Key Points:

- The slow La Niña and rapid El Niño decays are caused by differences in their anomalies over the subtropical and tropical Pacific
- The subtropical (tropical) anomalies activate a seasonal footprinting (thermocline variation) mechanism to affect the decay pace
- The asymmetric decay is projected to decrease in the future warming world due to the reduction of the subtropical anomaly difference

Supporting Information:

Supporting Information may be found in the online version of this article.

Correspondence to:

S. Chen and X. Wang, chensheng@scsio.ac.cn; wangxin@scsio.ac.cn

Citation:

Chen, J., Yu, J.-Y., Chen, S., Wang, X., Xiao, Z., & Fang, S.-W. (2022). Tropical and subtropical Pacific sources of the asymmetric El Niño-La Niña decay and their future changes. *Geophysical Research Letters*, 49, e2022GL097751. https://doi.org/10.1029/2022GL097751

Received 9 JAN 2022 Accepted 9 APR 2022

Author Contributions:

Conceptualization: Jiepeng Chen, Xin Wang

Data curation: Sheng Chen, Shih-Wei Fang

Formal analysis: Sheng Chen Funding acquisition: Jiepeng Chen, Jin-Yi Yu

Methodology: Jiepeng Chen Software: Sheng Chen

Supervision: Jin-Yi Yu, Xin Wang, Ziniu Xiao

Validation: Sheng Chen

Writing – original draft: Jiepeng Chen Writing – review & editing: Jin-Yi Yu, Sheng Chen, Xin Wang, Ziniu Xiao

© 2022. American Geophysical Union. All Rights Reserved.

Tropical and Subtropical Pacific Sources of the Asymmetric El Niño-La Niña Decay and Their Future Changes

Jiepeng Chen^{1,2,3,4,5} , Jin-Yi Yu⁵ , Sheng Chen^{1,3,4} , Xin Wang^{1,3,4} , Ziniu Xiao² , and Shih-Wei Fang⁵

¹State Key Laboratory of Tropical Oceanography, South China Sea Institute of Oceanology, Chinese Academy of Sciences, Guangzhou, China, ²State Key Laboratory of Numerical Modeling for Atmospheric Sciences and Geophysical Fluid Dynamics, Institute of Atmospheric Physics, Chinese Academy of Sciences, Beijing, China, ³Southern Marine Science and Engineering Guangdong Laboratory (Guangzhou), Guangzhou, China, ⁴Innovation Academy of South China Sea Ecology and Environmental Engineering, Chinese Academy of Sciences, Guangzhou, China, ⁵Department of Earth System Science, University of California, Irvine, CA, USA

Abstract El Niños (EN) are known to decay more rapidly, while La Niñas (LN) tend to decay more slowly. Observational analyses and coupled model experiments are conducted to show that sea surface temperature (SST) anomalies over the subtropical northeastern Pacific (SNEP) and equatorial western Pacific (EWP) are key factors to determine the decay pace of the EN and LN and their asymmetry. In the present climate the LN produces larger cold SST anomalies over the regions than the warm SST anomalies produced by the EN. The magnitude difference over the SNEP and EWP helps to slow down the LN decay via subtropical footprinting and tropical thermocline variation mechanisms, respectively. Coupled Model Intercomparison Project Phase 6 models project the magnitude differences of SNEP SST anomalies between EN and LN to reduce in the future warming world, causing the asymmetric EN-LN decay to weaken.

Plain Language Summary There are obvious asymmetric features in mature winter and decaying summer between the warm (El Niño [EN]) and cold phases (La Niña [LN]) of El Niño-Southern Oscillation (ENSO). Cold sea surface temperature (SST) anomalies over the subtropical northeastern Pacific (SNEP) and equatorial western Pacific (EWP) in winter are larger in amplitude during LN than EN. This asymmetric feature in winter enables the LN to delay slower and last longer than the EN in the following summer, which is another asymmetric feature between these two phases of the ENSO. The large cold anomalies over the SNEP can spread to the equatorial Pacific to slow down the LN decay through subtropical ocean-atmosphere coupling processes. The large cold anomalies over the EWP also contribute to the slow decay of LN but mainly through tropical ocean-atmosphere coupling processes. Climate models project that the future global warming may reduce the magnitude differences of the SNEP SST anomalies between EN and LN and cause a rapid decline of LN in a warmer world.

1. Introduction

The warm and cold phases (i.e., El Niño [EN] and La Niña [LN]) of the El Niño-Southern Oscillation (ENSO) exhibit notable asymmetric features not only in their spatial patterns (Dommenget et al., 2013; Hoerling et al., 1997) and peak intensities (An & Jin, 2004; Duan & Mu, 2006; Su et al., 2010) but also in their pace of decay (DiNezio & Deser, 2014; Guan et al., 2019; Hu et al., 2017; Okumura & Deser, 2010; W. Chen et al., 2014). Typically, EN and LN both develop in boreal summer, peak in winter, and decay in the following summer. However, the EN tends to exhibit a rapid decay, while the LN tends to decay slowly and, in some cases, even re-intensify in the following year to become multiyear events (Fang & Yu, 2020a; Kessler, 2002; McPhaden & Zhang, 2009; Santoso et al., 2017). The important impacts of the transition of ENSO decaying phases on the climate over the east Asia and western north Pacific attract more attention (J. Chen et al., 2018, 2018; 2020).

Several mechanisms have been proposed to explain the asymmetric decay between EN and LN. Some studies (e.g., Ohba & Ueda, 2009; Okumura & Deser, 2010; Okumura et al., 2011) emphasize the negative feedback provided by zonal wind anomalies in the far western equatorial Pacific to explain the asymmetric decay. Based on the western Pacific oscillator theory of ENSO (Weisberg & Wang, 1997), wind anomalies induced by the peak phase of the ENSO in this region can excite ocean Kelvin waves that later propagate to the eastern equatorial Pacific to terminate the ENSO event by bringing the anomalous thermocline back to normal. These studies argued

CHEN ET AL. 1 of 9



that the western Pacific winds respond asymmetrically to the sea surface temperature (SST) anomalies during the peak phase of EN and LN, which later lead to their asymmetric decay. Ohba and Ueda (2009), for example, demonstrated with ocean model experiments that a symmetric SST forcing over the tropical Pacific between EN and LN can generate asymmetric wind responses over the western Pacific, which can then lead to an asymmetric recovery of the thermocline over the equatorial eastern Pacific between these two phases of the ENSO.

Besides the nonlinear atmospheric feedback within the tropical Pacific, nonlinear feedbacks from the tropical Indian Ocean have also been suggested to be a contributing factor to the asymmetric decay. Ohba and Watanabe (2012) and Okumura et al. (2011) and indicated that the easterly anomalies in the equatorial western Pacific caused by the Indian Ocean basin warming during EN peak winter are much stronger than the westerly anomalies induced by the Indian Ocean basin cooling during LN peak winter, which can promote a faster termination of EN than LN. They verified this asymmetric Indian Ocean feedback to the asymmetric ENSO decay by prescribing Indian Ocean SST forcing in coupled model experiments. However, Chen M. et al. (2016) indicated that the basin-wide SST warming corresponding to zonal dipole pattern of observed rainfall anomalies in the Indian Ocean induces anomalous westerly winds in the EWP, which is opposite to the Indian Ocean SST forcing experiment with basin-wide rainfall anomaly. In contrast, the Atlantic feedbacks to ENSO is symmetric between EN and LN (L. Wang et al., 2017) and may reduce the asymmetry in ENSO decay (An & Kim, 2018).

In addition to atmospheric processes, oceanic processes also play a role in the ENSO decay asymmetry. Chen H. et al. (2016) suggested that a reversal in the equatorial zonal transport is more effective in terminating the EN than in terminating the LN. Hu et al. (2017) suggested that meridional gradient of thermocline and off-equatorial sea surface height anomaly also contribute to the asymmetric decay between EN and LN. Guan et al. (2019) emphasized the mean thermocline depth across the equatorial Pacific in determining the asymmetry EN and LN durations. Most of these earlier studies considered the contributions of asymmetric oceanic processes to the ENSO transition asymmetry from the charged-discharged mechanism of the ENSO dynamics. It is noted that the charged-discharged mechanism has become less dominant in determining ENSO variability after 2,000, in concurrent with an increase occurrence of central Pacific EN events (McPhaden, 2012; Neske & McGregor, 2018; Yu et al., 2012). Aside from the charged-discharged mechanism, the seasonal footprinting mechanism (Vimont et al., 2003) that emphasizes subtropical Pacific air-sea interactions is another important mechanism to determine ENSO variability and was suggested to play an important role in contributing to ENSO complexity (X. Wang et al., 2019a, 2019b; Yu & Fang, 2018). However, it is not yet clear how the subtropical air-sea coupling processes may affect the asymmetric decay between EN and LN. In this study, we explore the role of subtropical Pacific coupling processes associated with the seasonal footprinting mechanism in the asymmetric decay between EN and LN. Furthermore, the possible change in the asymmetric EN-LN decay due to global warming is investigated using Coupled Model Intercomparison Project Phase 6 (CMIP6) models.

2. Data Sets and Methods

For the observations, this study uses monthly mean atmospheric data from the National Centers for Environmental Prediction/National Center for Atmospheric Research Reanalysis 1 (NCEP/NCAR-R1) at a resolution of $2.5^{\circ} \times 2.5^{\circ}$ (Kalnay et al., 1996). Monthly SST data is from the Extended Reconstructed SST version 5 at a resolution of $2^{\circ} \times 2^{\circ}$ (Huang et al., 2017). Monthly SSH data is from the German contribution of the Estimating the Circulation and Climate of the Ocean project at a resolution of $1^{\circ} \times 1^{\circ}$ (Köhl, 2015). The analysis period of this study is from January 1950 to December 2020. Anomalies are defined as departures from the climatological seasonal cycle averaged over the analysis period after removing linear trends. To project the future change in the asymmetric ENSO decay and the inter-model variability of the projection, we utilize the historical simulations and Shared Socioeconomic Pathway 5–8.5 (SSP5-8.5) emission scenarios produced by 19 CMIP6 models (see Table S1 in the Supporting Information S1 for details). The recent 65-year integrations from 1950 in the historical simulations and the last 65 years from 2036 in the SSP5-8.5 simulations were used for analyses.

Following the NOAA/National Weather Service/Climate Prediction Center, an EN (LN) event is identified when the three-month running mean value of Niño3.4 (170°W–120°W and 5°S–5°N) SST anomalies are larger than 0.5°C (smaller than –0.5°C) for at least 5 consecutive overlapping seasons. A total of 25 EN events and 22 LN events were selected during 1950–2020 (See Text S1 and Table S2 in Supporting Information S1). Following Yu and Fang (2018), a Multi-variate Empirical Orthogonal Function (MEOF) analysis is used to identify the

CHEN ET AL. 2 of 9

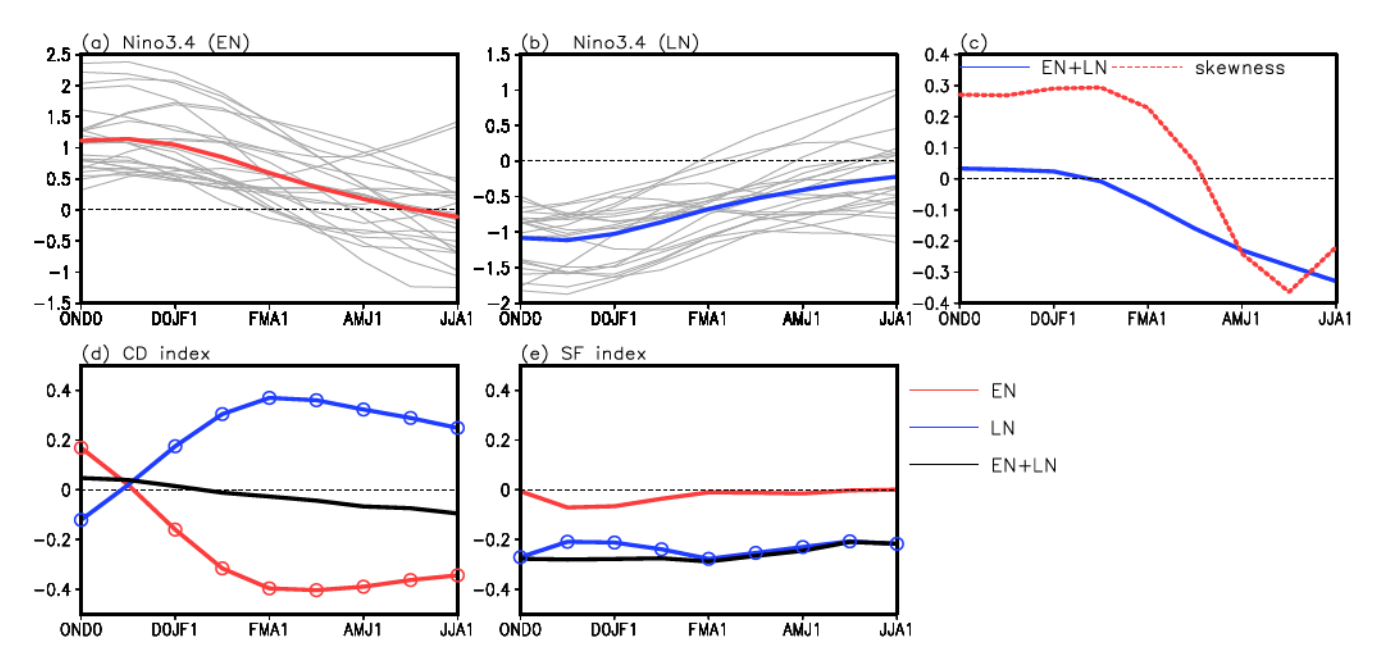


Figure 1. Temporal evolutions of Niño3.4 indices (°C) for the composite (a) El Niño (EN) events (EN, thick red line) and (b) La Niña (LN) (thick blue line) events and the individual events (gray lines) comprising the composites. (c) The EN-LN asymmetry in the composite Niño3.4 evolutions (blue line; estimated as the summation of the two composite evolutions in a and b) and the intensity of the asymmetry (red line; estimated as the skewness of the ENSO events). Temporal evolutions of the intensity of (d) the charged-discharged mechanism (CD) and (e) the seasonal footprinting mechanism (SF) composited for the EN (red line) and LN events (blue line). Also shown in the panel is their asymmetric component (black line). Empty circles in (d), (e) indicate the differences significant at the 90% confidence level, based on the two-tailed Student's £test. On the abscissa, "0" and "1" refer to the developing and decaying years of EN/LN events, respectively.

charged-discharged and seasonal footprinting mechanisms and their strengths. The MEOF analysis was applied to the combined anomalies in SSTs, SSHs, and surface winds over the tropical Pacific (122°E–70°W and 20°S–20°N) for the period 1948–2017 (see Text S2 in Supporting Information S1 for details). The second and third MEOF modes represent the seasonal footprinting and charged-discharged mechanisms, respectively, and their corresponding principal components are used to quantify the strengths and phases of the mechanisms. The EWP region is defined as the area between 150° and 180°E and 5°S–5°N, whereas the subtropical northeastern Pacific (SNEP) is defined as the area between 145°W and 115°W and 15°–25°N. Asymmetries between EN and LN are quantified as the sums of EN and LN composites following previous studies (e.g., Chen, Hu, et al., 2016; Hu et al., 2017; W. Chen et al., 2014). The skewness of the EN and LN events is calculated to quantify the intensity of asymmetries (e.g., An et al., 2005; An & Jin, 2004; Burgers & Stephenson, 1999). A series of numerical experiments were conducted in this study with the Community Earth System Model Version 1.2.2 (CESM1.2.2) from the National Center for Atmospheric Research (See Text S3 in Supporting Information S1 for the details of the model configurations).

3. Results

3.1. Asymmetric SST Evolution Patterns Between El Niño and La Niña

Figures 1a and 1b show the evolutions of Niño3.4 SST index composited for the EN and LN from their mature winter to subsequent summer. Also shown in the figures are the evolutions for the individual events that comprise the composites. The composite evolution for EN shows a rapid decline of the Niño3.4 SST index after winter and changes to an opposite sign in the following summer. This fast decay can be seen in 15 of the 25 EN events (i.e., 60%) occurred during 1950–2020. Conversely, the composite evolution of the LN shows a slow decay of the Niño3.4 SST index with its negative value persists into the following year. This slow decay can be seen in most of the LN events (i.e., 14 out of the 22 LN events; 63.6%) that occurred during 1950–2020. The asymmetry between the decay pace of EN and LN is evident during the analysis period. We quantify the asymmetry and its intensity in Figure 1c by calculating the sum and skewness of the EN and LN composites. This figure indicates that the

CHEN ET AL. 3 of 9



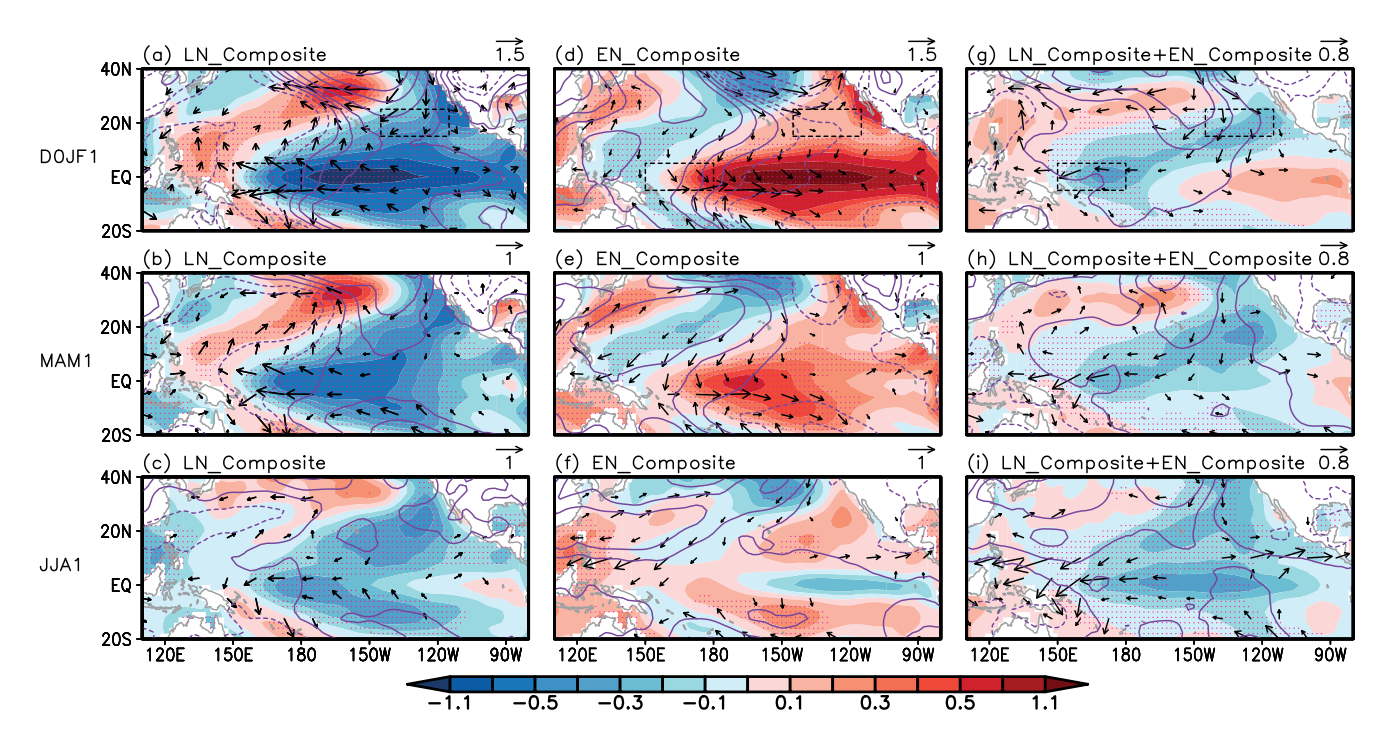


Figure 2. Composite anomalies of sea surface temperature (SST) (shading, $^{\circ}$ C), 1,000 hPa winds (vector, m s⁻¹), and sea level pressure (contour, hPa) for the La Niña events (a–c), the El Niño events (d–f), and the asymmetries between them (g–i). The evolutions of the anomalies are shown from the peak winter (the top row) to the following spring (the middle row) and summer (the bottom row). Dotted areas in (a–f) denote SST anomalies above the 90% confidence level. Only composite wind anomalies exceeding the 90% confidence level are plotted in (a–f). Wind anomalies less than 0.2 m s⁻¹ are omitted. Skewness of the asymmetry less than -0.3 are dotted in (g–i). Contours are plotted for the anomaly values of \pm 0.2, \pm 0.4, \pm 0.8, \pm 1.4, \pm 2, and \pm 3 in their corresponding units. On the ordinate, "0" and "1" refer to the developing and decaying years of the El Niño-Southern Oscillation events, respectively. The right black box in (a, d, and g) denotes the subtropical northeastern Pacific (145°W-115°W and 15°-25°N) region, whereas the left black box denotes the equatorial western Pacific (150°-180°E and 5°S-5°N) region.

asymmetry is particularly evidenced in the decaying summer, where large negative values of sum and skewness of Niño3.4 SST index appear.

To explore the relative contributions of the charged-discharged and seasonal footprinting mechanisms to the asymmetric EN-LN decay, the temporal evolutions of the intensities of these two mechanisms during the EN and LN events are also separately composited and displayed in Figures 1d and 1e. For the charged-discharged mechanism, it has negative values after the peak winter for the EN and positive values for LN, contributing to a fast decay of both the EN and LN (Figure 1d). The magnitude of this mechanism is comparable between EN and LN, despite a slightly larger magnitude in the former than in the latter. This is consistent with previous papers (Guan et al., 2019; Hu et al., 2017). In contrast, the composite intensity of the seasonal footprinting mechanism is much larger during the LN than during the EN (Figure 1e). This subtropical coupling mechanism has a larger influence on the decay of LN than on the decay of EN. Interestingly, it has negative values for both the EN and LN meaning that this mechanism tends to damp the EN but to maintain the LN. Figures 1d and 1e together suggest that the seasonal footprinting mechanism plays a more dominant role than the charge-discharged mechanism in causing the asymmetric decay between EN and LN.

To identify the physical processes that activate the seasonal footprinting mechanism during ENSO to produce the asymmetric decay, we further contrasted the composite atmospheric and oceanic anomalies between EN and LN to examine their asymmetries (Figure 2). In the LN composite, an anomalous anticyclone is evident over the SNEP and persists during the peak winter (Figure 2a). The anomalous northeasterlies in the southeastern flank of the anticyclone, coupled with cold SST anomalies underneath, gradually extend into the equator in the decaying spring and maintain themselves over the central equatorial Pacific through the decaying summer (Figures 2b and 2c). The anomalous anticyclone is part of the Pacific–North American (PNA) teleconnection (Wallace & Gutzler, 1981) typically excited by the anomalous heating produced by the ENSO (Guo et al., 2015; Soulard et al., 2019). In contrast, the EN composites (Figures 2d–2f) indicate that the anomalous northeastern Pacific cyclone produced during the peak winter of EN weakens rapidly in the following spring and summer.

CHEN ET AL. 4 of 9



The asymmetric atmospheric circulation responses between EN and LN can be attributed to different SST anomalies they produce over the SNEP. It is apparent from Figure 2 that LN produces larger SST anomalies over the SNEP than EN during their peak winters. Hoerling et al. (1997) suggested that the PNA teleconnection excited by LN exhibits a westward shift pattern compared to that excited by El Niño due to a similar westward displacement in anomalous deep convection in the tropical Pacific. Over the SNEP, the La Nina-induced anomalous anticyclone is located west of the EN-induced anomalous cyclone. This enables La Nina to produce stronger anomalous trade winds and cause stronger coastal upwelling and wind-evaporation-SST feedback than EN. As a result, the cold SST anomalies induced by La Nina over the SNEP are larger than the warm SST anomalies induced by EN. The asymmetry in the SST responses (Figure 2g) is the largest over the SNEP, where the seasonal footprinting mechanism originates. We find that this asymmetric SST response is accompanied with an asymmetry in the 500 hPa vertical velocity (see Figure S1 in Supporting Information S1). It indicates that the anomalous cooling induced by the LN over the SNEP is stronger than the anomalous heating induced by the EN. Therefore, the LN is more capable than the EN in exciting atmospheric circulation anomalies over the SNEP, which is also evident in the positive SLP asymmetry shown in Figures 2g-2i. The stronger cold anomaly over the SNEP couples with the stronger anomalous anticyclone to its west (see Figures 2a and 2b) to extend the cold anomalies southwestward into the equatorial central Pacific. This strong seasonal footprinting mechanism helps to maintain the LN condition through the decaying summer (Figure 2). The seasonal footprinting mechanism is weak during the EN due to the weak SST anomalies it produces over the SNEP. Therefore, the EN decays faster during the decaying summer (Figures 2d-2f).

As mentioned, zonal winds over the EWP also respond asymmetrically to EN and LN SST anomalies (e.g., Okumura & Deser, 2010; Song et al., 2022). This is another region in Figure 2g that exhibits large and significant asymmetries between EN and LN during their peak winter. Negative values appear over the region for both the SST and wind asymmetries, meaning that the anomalous cold SSTs and easterlies produced by the LN (Figure 2a) are stronger than the anomalous warm SSTs and westerlies produced by the EN (Figure 2b). The asymmetries persist from the peak winter to the following spring and summer (Figures 2h and 2i). Okumura and Deser (2010) indicated that the stronger wind response over the EWP during LN than during EN results from a westward shift of the atmospheric response to their SST anomalies during peak winter. Because of this westward-shift, the easterly anomalies over the EWP during La Nina's decaying season are strong enough to counteract the westerly anomalies induced by the anomalous cyclone over the northwestern Pacific. In contrast, during EN's decaying season, the westerly anomalies over the EWP balance the easterly anomalies induced by the anomalous anticyclone over the northwestern Pacific. As shown in Figures 2a-2c, the LN-induced strong cold SST anomalies and strong easterly anomalies over the EWP coupled with each other to persist from winter to summer. The strong easterly anomalies during the decaying phase of the LN can force upwelling oceanic equatorial Kelvin waves propagating eastward to help maintain cold SST anomalies over the eastern Pacific (An & Kim, 2018; Okumura & Deser, 2010; Weisberg & Wang, 1997), leading to a prolongation of LN into the next year. In contrast, the EN-induced weak warm SST anomalies and weak westerly anomalies decline quickly after the peak winter and cannot help to maintain warm SST anomalies over the eastern Pacific (Figures 2d-2f). It should be noted that, as a result of larger nonlinear dynamical heating, EN has larger SST anomalies in the equatorial eastern-to-central Pacific than LN (Duan et al., 2013; Duan & Mu, 2006). The nonlinear dynamical heating associated with SST anomalies in this region may also cause fast decay of extreme EN (Duan et al., 2009; Wu & Duan, 2012), contributing to asymmetric decays between EN and LN to some extent.

3.2. Respective Contributions of the SNEP and EWP SST Anomalies to the Asymmetric Decay Between El Niño and La Niña

Our analyses indicate that the contrasting SST anomalies over the SNEP and EWP regions and their associated atmospheric circulation responses are two key factors contributing to the asymmetric decay between EN and LN. To identify their respective contributions to the rapid decay of EN and long persistence of LN, we conducted three sets of 20-member ensemble experiments with the CESM1.2.2: the Control, SNEP, and EWP experiments. We first conducted a 1200-year preindustrial simulation with the CESM1.2.2 and used the last 200 years to calculate the model climatology. In the ensemble Control experiment, its 20 members are integrated from the different initial atmospheric conditions of the LN-EN transition event. The ensemble SNEP experiment was conducted in a similar way as the Control experiment, except that a Gaussian-shaped negative SST anomaly from December to following February was imposed in the SNEP region (Figure S2a in Supporting Information S1). A similar SST

CHEN ET AL. 5 of 9



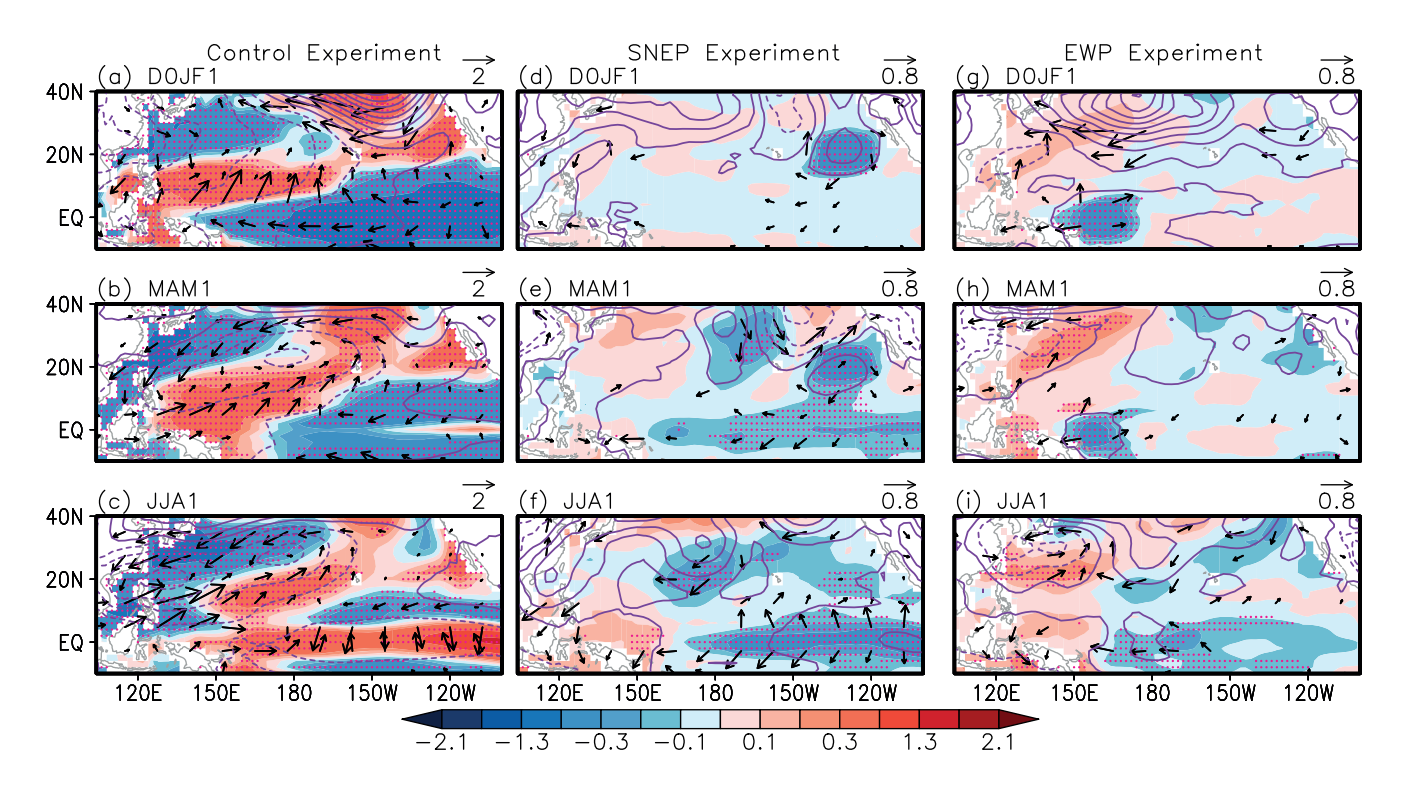


Figure 3. The differences between the ensemble means of the Control experiment and the climatology of the Pre-Industrial simulation in ocean temperature at 5m (used as a proxy for sea surface temperature [SST]; shading, $^{\circ}$ C), sea level pressure (contour, hPa), and 992 hPa winds (vector, m s⁻¹) from the peak winter (a) to the following spring (b) and summer (c). Panels (d–f) show the ensemble mean differences between the subtropical northeastern Pacific and Control experiments, whereas (g–i) show the differences between the equatorial western Pacific and Control experiments. Dotted areas denote SST differences above the 90% confidence level. Only composite wind differences exceeding the 90% confidence level are plotted. Contour interval is 0.5 in (a–c) and 0.2 in (d–i). On the ordinate, "0" and "1" refer to the developing and decaying years of the El Niño-Southern Oscillation events, respectively.

anomaly was imposed in the EWP region for the ensemble EWP experiment (Figure S2b in Supporting Information S1). The imposed SST anomalies have an intensity in region average of -0.3° C, which were determined based on the winter SST anomaly asymmetry shown in Figure 2c. Each set of experiments has 20 members and each member is integrated from a December initial condition to November of the following year.

Figures 3a–3c show the differences between the ensemble mean calculated from the Control experiment and the climatology of the Pre-Industrial simulation. As expected, the anomalies (i.e., the differences) in the Control experiment show a transition from a LN in its peak winter to an EN in the following summer. Compared to the Control experiment, the SNEP experiment confirms that the cold SNEP SST anomalies in winter contribute to significantly prolong the LN duration into the following spring and summer through the seasonal footprinting mechanism (Figures 3d–3f). The cold SNEP SST anomalies induce an anomalous anticyclone, which produces lower-level northeasterly anomalies on its northeastern flank to enhance the climatological trade winds and local surface evaporation. The wind-evaporation-SST feedback (Xie & Philander, 1994) grows and expands the cold SNEP SST anomalies southwestward into the equatorial central Pacific during the decaying spring. The cold SST anomalies in the equatorial central and eastern Pacific get amplified further by Bjerknes feedback (Bjerknes, 1969) and help maintain the LN condition into summer.

In the EWP experiments, significant easterly anomalies occur in the far western equatorial Pacific as a direct response to the imposed cold EWP SST forcing in winter (Figure 3g). The anomalous easterlies persist into the following spring and summer, prohibiting the recovery of the thermocline slope and thus help to prolong the LN in the decaying summer (Figures 3h and 3i). This experiment confirms that the larger cold SST anomalies in the EWP enable the LN to decay slower than the El Niño through tropical oceanic dynamical processes portrayed by the western Pacific oscillator (Weisberg & Wang, 1997). By comparing the EWP and SNEP experiments, we notice that the EWP SST forcing has a weaker contribution than the SNEP SST forcing to the maintenance of the cold SST anomalies in the equatorial central-to-eastern Pacific in subsequent summer (cf. Figures 3i and 3f). It is interesting to note that the cold EWP SST anomalies can also trigger an anomalous anticyclone and cold SST

CHEN ET AL. 6 of 9

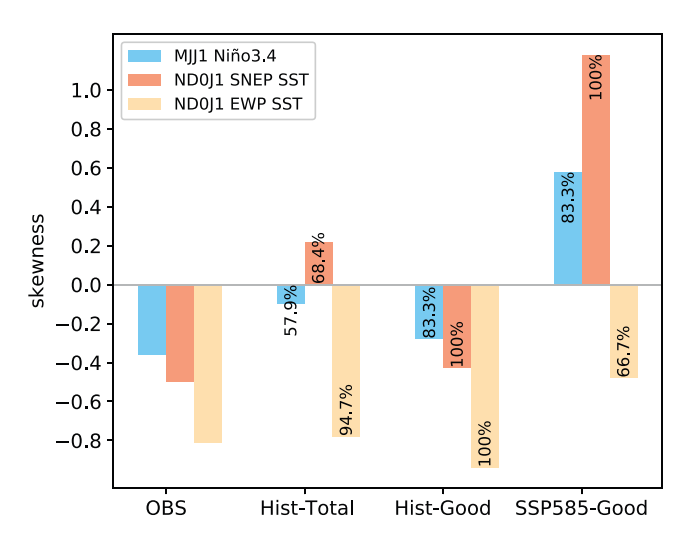


Figure 4. The skewness of sea surface temperature (SST) anomalies over the subtropical northeastern Pacific (SNEP) (orange bar) and equatorial western Pacific (yellow bar) in November-December-January and the skewness of SST anomalies over the Niño3.4 region (blue bar) in the following May-June-July during El Niño-Southern Oscillation events. The skewness is calculated from the observations (OBS) and the ensemble means of the historical simulations from the 19 Coupled Model Intercomparison Project Phase 6 (CMIP6) models listed in Table S1 (Hist-Total), the 6 CMIP6 models in which the skewness of the SNEP SST anomalies in November-December-January is negative (Hist-Good), and the SSP5-8.5 simulations with these 6 CMIP6 models (SSP585-Good). The numbers on the bars denote the percentage of the models that produce same signs of skewness. On the label, "0" and "1" refer to the developing and decaying years of El Niño/La Niña events, respectively.

anomalies over the SNEP region. This result confirms the suggestion from Fang and Yu (2020b) that SST anomalies over the tropical western-to-central Pacific can excite an atmospheric wave train propagating northward to induce SNEP SST anomalies and to trigger the seasonal footprinting mechanism. However, the induced SNEP SST anomalies are not strong enough to extend the subtropical cold SST anomalies into the equator in the following seasons (Figure 3h). Our results suggest that the EWP SST anomalies can affect the pace of the ENSO decay through both the tropical thermocline mechanism and the subtropical footprinting mechanism, although the former appears to be more important than the latter. These three sets of experiments demonstrate that the stronger SNEP and EWP SST anomalies during LN than EN at their peak winter are key factors to cause the asymmetric ENSO decay through subtropical and tropical Pacific processes, respectively.

3.3. Future Changes in the Asymmetric Decay Between El Niño and La Niña

We select a group of six good models (referred to as "Hist-Good" in Figure 4; see Table S1 in Supporting Information S1) from the 19 CMIP6 models to examine their projections under high emissions scenario (SSP5-8.5; referred to SSP585-Good; hereafter). These six models are capable of simulating the negative asymmetry in SNEP and EWP SST anomalies during the peak winter of ENSO in the historical simulation, similar to the observations. The SSP585-Good models consistently project the SNEP SST skewness to sharply increase and turn positive in the future warming world, while more than half of the models project the EWP SST skewness to slightly increase but remain negative. The projected change of the Niño3.4 skewness in the decaying summer has the same sign of the change in the SNEP SST skewness in the peak winter. This result indicates that the future change in the asym-

metric ENSO decay is likely to be dominant by the influence from the SNEP SST anomalies than the influence from the EWP SST.

In the observation, the asymmetric decay of ENSO (i.e., the negative skewness of Niño3.4 SST anomalies during the ENSO decaying summer) is a result of the fast decay of EN and the slow decay of LN. In the SSP5-8.5 projections, the positive skewness of Niño3.4 SST anomalies during the ENSO decaying summer may be caused by a slow decay of EN or a fast decay of LN. Yun et al. (2019) proposed the EN-to-LN transition is unchanged under global warming. The nonlinear dynamical heating along the equatorial Pacific thermocline is essential for the generation of strong EN events (Hayashi et al., 2020; Jin et al., 2003). Strong EN events tend to decay rapidly, as a result of the large nonlinear dynamical heating (Duan et al., 2009; Wu & Duan, 2012). As global temperatures warm, the nonlinear dynamical heating becomes negligible for strong EN (Kohyama & Hartmann, 2017). However, Fang and Yu (2020b) suggested the occurrence of cyclic ENSO transitions (i.e., rapid transitions between EN and LN) to increase and the occurrence of multiyear ENSO transitions (i.e., slow transitions) to decrease in the future warming world. They imply the decay rate of LN may be speeded up due to global warming. By evaluating the evolution of the multi-model-mean Niño3.4 SST anomalies from the SSP585-Good models (Figure S3 in Supporting Information S1), we find that both the EN and LN exhibit a fast decay after their mature winter, which explains the reduced asymmetry in ENSO decay. It can be concluded that the SNEP SST forcing play a crucial role in controlling the ENSO decay asymmetry.

4. Summary and Discussion

The present study identifies the SNEP and EWP as the two key regions where their SST anomalies play a critical role in controlling the asymmetric decay between EN and LN. SST anomalies over the SNEP and EWP regions can activate subtropical Pacific coupling processes (i.e., the seasonal footprinting mechanism) and tropical oceanic dynamical processes (i.e., related to western Pacific oscillator), respectively, to control the decay pace of ENSO (Figure S4 in Supporting Information S1). In the present climate, the larger SST anomalies produced by

CHEN ET AL. 7 of 9



the LN over these two regions than EN cause the LN to decay slowly and the EN to decay rapidly. CMIP6 models project that, in the future warming world, the asymmetry in ENSO decay may decrease due to a reduction of the difference between the EN and LN in the magnitudes of their SNEP SST anomalies. This study has identified a key source for EN-LN asymmetries in their evolutions and durations that can be further explored to improve extended ENSO predictions and future projections. Future studies are needed to explain how and why the EN and LN produce asymmetric of SST anomalies over the SNEP and EWP.

Data Availability Statement

All data and numerical model used in this study are publicly accessible. The Extended Reconstructed SST in version 5 were downloaded from their website (https://psl.noaa.gov/data/gridded/data.noaa.ersst.v5.html). The atmospheric variables of NCEP/NCAR-R1 were obtained from NOAA (https://psl.noaa.gov/data/gridded/data.ncep.reanalysis.html). The SSH in the German contribution of the Estimating the Circulation and Climate of the Ocean project were downloaded from the Integrated Climate Data Center (https://www.cen.uni-hamburg.de/en/icdc/data/ocean/easy-init-ocean/gecco2.html). All CMIP6 data are available at the Earth System Grid Federation (ESGF; https://esgf-node.llnl.gov/projects/cmip6) after registration. We acknowledge the following numerical model information providers: CESM1.2.2 (https://www.cesm.ucar.edu/models/cesm1.2/). The model data output used in this study can be accessed at Zenodo with DOI: https://doi.org/10.5281/zenodo.6416175.

Acknowledgments References

This research is jointly supported by the

National Key Research and Development

Program of China (2020YFA0608803),

the Strategic Priority Research Program

(XDB42000000 and XDA20060502),

of China (41925024 and 41876021),

the Key Special Project for Introduced

the National Natural Science Foundation

Talents Team of Southern Marine Science

and Engineering Guangdong Laboratory

Guangdong Natural Science Foundation

China (202102020384), the Independent

Research Project Program of State Key

Laboratory of Tropical Oceanography

(LTOZZ2005, LTOZZ2201), and the open

fund of State Key Laboratory of Numer-

ical Modeling for Atmospheric Sciences

Institute of Atmospheric Physics, Chinese

Academy of Sciences. Jin-Yi Yu acknowl-

National Science Foundation under grants

AGS-1833075 and AGS-2109539, Sheng

Chen acknowledges the support from the

National NSFC (42006033). All numeri-

cal simulations are supported by the High

HPC managers of Wei Zhou and Dandan

Performance Computing Division and

Sui in the South China Sea Institute

of Oceanology, Chinese Academy of

Sciences

edges the support from the Climate and

Large-Scale Dynamics Program of the

and Geophysical Fluid Dynamics,

(Guangzhou; GML2019ZD0306), the

(2021A1515011368), the Science and

Technology Program of Guangzhou

of Chinese Academy of Sciences

- An, S.-I., Ham, Y.-G., Kug, J.-S., Jin, F.-F., & Kang, I.-S. (2005). El Niño-La Niña asymmetry in the coupled model intercompares on project simulations. *Journal of Climate*, 18(14), 2617–2627. https://doi.org/10.1175/JCLI3433.1
- An, S.-I., & Jin, F.-F. (2004). Nonlinearity and asymmetry of ENSO. *Journal of Climate*, 17(12), 2399–2412. https://doi.org/10.1175/1520-0442(2004)017(2399:NAAOE)2.0.CO;2
- An, S.-I., & Kim, J.-W. (2018). ENSO transition asymmetry: Internal and external causes and Intermodel diversity. Geophysical Research Letters, 45(10), 5095–5104. https://doi.org/10.1029/2018GL078476
- Bjerknes, J. (1969). Atmospheric teleconnections from the equatorial Pacific. *Monthly Weather Review*, 97(3), 163–173. https://doi.org/10.1175/1520-0493(1969)097<0163:ATFFFP>2.3.CO:2
- Burgers, G., & Stephenson, D. B. (1999). The "Normality" of El Niño. Geophysical Research Letters, 26(8), 1027–1030. https://doi. org/10.1029/1999GL900161
- Chen, H. C., Hu, Z. Z., Huang, B., & Sui, C. H. (2016). The role of reversed equatorial zonal transport in terminating an ENSO event. *Journal of Climate*, 29(16), 5859–5877. https://doi.org/10.1175/JCLI-D-16-0047.1
- Chen, J., Wang, X., Zhou, W., Wang, C., Xie, Q., Li, G., & Chen, S. (2018). Unusual rainfall in southern China in decaying August during extreme El Niño 2015/16: Role of the western Indian Ocean and North tropical Atlantic SST. *Journal of Climate*, 31(17), 7019–7034. https://doi.org/10.1175/ICLJ-D-17-0827.1
- Chen, J., Wang, X., Zhou, W., & Wen, Z. (2018). Interdecadal change in the summer SST-precipitation relationship around the late 1990s over the South China Sea. Climate Dynamics, 51(5–6), 2229–2246. https://doi.org/10.1007/s00382-017-4009-y
- Chen, J., Yu, J.-Y., Wang, X., & Lian, T. (2020). Different influences of southeastern Indian Ocean and Western Indian Ocean SST anomalies on eastern China rainfall during the decaying summer of 2015/16 extreme El Niño. *Journal of Climate*, 33(13), 5427–5443. https://doi. org/10.1175/JCLI-D-19-0777.1
- Chen, M., Li, T., Shen, X., & Wu, B. (2016). Relative roles of dynamic and thermodynamic processes in causing evolution asymmetry between El Niño and La Niña. *Journal of Climate*, 29(6), 2201–2220. https://doi.org/10.1175/JCLI-D-15-0547.1
- Chen, W., Lu, R.-Y., & Dong, B. (2014). Revisiting asymmetry for the decaying phases of El Niño and La Niña. Atmospheric and Oceanic Science Letters, 7(4), 275–278. https://doi.org/10.3878/j.issn.1674-2834.13.0091
- DiNezio, P. N., & Deser, C. (2014). Nonlinear controls on the persistence of La Niña. Journal of Climate, 27(19), 7335–7355. https://doi. org/10.1175/JCLI-D-14-00033.1
- Dommenget, D., Bayr, T., & Frauen, C. (2013). Analysis of the non-linearity in the pattern and time evolution of El Niño southern oscillation. Climate Dynamics, 40(11–12), 2825–2847. https://doi.org/10.1007/s00382-012-1475-0
- Duan, W., & Mu, M. (2006). Investigating decadal variability of El Nino-Southern Oscillation asymmetry by conditional nonlinear optimal
- perturbation. Journal of Geophystcal Research, 111, C07015. https://doi.org/10.1029/2005JC003458

 Duan, W., Xue, F., & Mu, M. (2009). Investigating a nonlinear characteristic of El Niño events by conditional nonlinear optimal perturbation.
- Atmospheric Research, 94(1), 10–18. https://doi.org/10.1016/j.atmosres.2008.09.003

 Duan, W., Yu, Y., Xu, H., & Zhao, P. (2013). Behaviors of nonlinearities modulating El Nino events induced by optimal precursory disturbance.
- Climate Dynamics, 40(5–6), 1399–1413. https://doi.org/10.1007/s00382-012-1557-z
 Fang, S.-W., & Yu, J.-Y. (2020a). Contrasting transition complexity between El Niño and La Niña: Observations and CMIP5/6 models. Geophysical Research Letters, 47, e2020GL088926. https://doi.org/10.1029/2020GL088926
- Fang, S.-W., & Yu, J.-Y. (2020b). A control of ENSO transition complexity by tropical Pacific mean SSTs through tropical-subtropical interaction. Geophysical Research Letters, 47(12), e2020GL087933. https://doi.org/10.1029/2020GL087933
- Guan, C., McPhaden, M. J., Wang, F., & Hu, S. (2019). Quantifying the role of oceanic feedbacks on ENSO asymmetry. Geophysical Research Letters, 46(4), 2140–2148. https://doi.org/10.1029/2018GL081332
- Guo, Y., Wen, Z., Wu, R., Lu, R., & Chen, Z. (2015). Impact of tropical Pacific precipitation anomaly on the East Asian upper-tropospheric westerly jet during the boreal winter. *Journal of Climate*, 28(16), 6457–6474. https://doi.org/10.1175/JCLI-D-14-00674.1
- Hayashi, M., Jin, F., & Stuecker, M. (2020). Publisher correction: Dynamics for El Niño-La Niña asymmetry constrain equatorial-Pacific warming pattern. Nature Communications, 11(1), 4672. https://doi.org/10.1038/s41467-020-18650-y

CHEN ET AL. 8 of 9



- Hoerling, M. P., Kumar, A., & Zhong, M. (1997). El Niño, La Niña, and the nonlinearity of their teleconnections. *Journal of Climate*, 10(8), 1769–1786. https://doi.org/10.1175/1520-0442(1997)010<1769
- Hu, Z.-Z., Kumar, A., Huang, B., Zhu, J., Zhang, R.-H., & Jin, F.-F. (2017). Asymmetric evolution of El Niño and La Niña: The recharge/discharge processes and role of the off-equatorial sea surface height anomaly. Climate Dynamics, 49(7–8), 2737–2748. https://doi.org/10.1007/s00382-016-3498-4
- Huang, B., Thorne, P. W., Banzon, V. F., Boyer, T., Chepurin, G., Lawrimore, J. H., et al. (2017). Extended reconstructed sea surface temperature version 5 (ERSSTv5), upgrades, validations, and intercomparisons. *Journal of Climate*, 30(20), 8179–8205. https://doi.org/10.1175/JCLI-D-16-0836.1
- Jin, F.-F., An, S.-I., Timmermann, A., & Zhao, J. (2003). Strong El Niño events and nonlinear dynamical heating. Geophysical Research Letters, 30(3), 1120. https://doi.org/10.1029/2002GL016356
- Kalnay, E., Kanamitsu, M., Kistler, R., Collins, W., Deaven, D., Gandin, L., et al. (1996). The NCEP/NCAR 40-year reanalysis project. Bulletin of the American Meteorological Society, 77(3), 437–472. https://doi.org/10.1175/1520-0477(1996)077<0437:TNYRP>2.0
- Kessler, W. S. (2002). Is ENSO a cycle or a series of events? Geophysical Research Letters, 29(23), 2125. https://doi.org/10.1029/2002GL015924
 Köhl, A. (2015). Evaluation of the GECCO2 ocean synthesis: Transports of volume, heat and freshwater in the Atlantic. Quarterly Journal of the Royal Meteorological Society, 141(686), 166–181. https://doi.org/10.1002/qj.2347
- Kohyama, T., & Hartmann, D. (2017). Nonlinear ENSO warming suppression (NEWS). Journal of Climate, 30(11), 4227–4251. https://doi.org/10.1175/JCLI-D-16-0541.1
- McPhaden, M. J. (2012). A 21st century shift in the relationship between ENSO SST and warm water volume anomalies. Geophysical Research Letters, 39(9), L09706. https://doi.org/10.1029/2012GL051826
- McPhaden, M. J., & Zhang, X. (2009). Asymmetry in zonal phase propagation of ENSO sea surface temperature anomalies. Geophysical Research Letters, 36(13), L13703. https://doi.org/10.1029/2009GL038774
- Neske, S., & McGregor, S. (2018). Understanding the warm water volume precursor of ENSO events and its interdecadal variation. Geophysical Research Letters, 45(3), 1577–1585. https://doi.org/10.1002/2017GL076439
- Ohba, M., & Ueda, H. (2009). Role of nonlinear atmospheric response to SST on the asymmetric transition process of ENSO. *Journal of Climate*, 22(1), 177–192. https://doi.org/10.1175/2008JCLI2334.1
- Ohba, M., & Watanabe, M. (2012). Role of the Indo-Pacific interbasin coupling in predicting asymmetric ENSO transition and duration. *Journal of Climate*, 25(9), 3321–3335. https://doi.org/10.1175/JCLI-D-11-00409.1
- Okumura, Y. M., & Deser, C. (2010). Asymmetry in the duration of El Niño and La Niña. Journal of Climate, 23(21), 5826-5843. https://doi.org/10.1175/2010JCLI3592.1
- Okumura, Y. M., Ohba, M., Deser, C., & Ueda, H. (2011). A proposed mechanism for the asymmetric duration of El Niño and La Niña. *Journal*
- of Climate, 24(15), 3822–3829. https://doi.org/10.1175/2011JCLI3999.1

 Santoso, A., McPhaden, M. J., & Cai, W. (2017). The defining characteristics of ENSO extremes and the strong 2015/2016 El Niño. Reviews of
- Geophysics, 55(4), 1079–1129. https://doi.org/10.1002/2017RG000560
 Song, X., Zhang, R., & Rong, X. (2022). Dynamic causes of ENSO decay and its asymmetry. Journal of Climate, 35(2), 445–462. https://doi.
- org/10.1175/JCLI-D-21-0138.1

 Soulard, N., Lin, H., & Yu, B. (2019). The changing relationship between ENSO and its extratropical response patterns. *Scientific Reports*, 9, 6507. https://doi.org/10.1038/s41598-019-42922-3
- Su, J., Zhang, R., Li, T., Rong, X., Kug, J.-S., & Hong, C.-C. (2010). Causes of the El Niño and La Niña amplitude asymmetry in the equatorial eastern Pacific. *Journal of Climate*, 23(3), 605–617. https://doi.org/10.1175/2009JCL12894.1
- Vimont, D. J., Wallace, J. M., & Battisti, D. S. (2003). The seasonal footprinting mechanism the Pacific: Implications for ENSO. *Journal of Climate*, 16(16), 2668–2675. https://doi.org/10.1175/1520-0442(2003)016<2668:TSFMIT>2.0.CO
- Wallace, J. M., & Gutzler, D. S. (1981). Teleconnections in the geopotential height field during the Northern Hemisphere winter. Monthly Weather Review, 109(4), 784–812. https://doi.org/10.1175/1520-0493(1981)109<0784:TITGHF>2.0
- Wang, X., Chen, M., Wang, C., Yeh, S.-W., & Tan, W. (2019a). Evaluation of performance of CMIP5 models in simulating the North Pacific oscillation and El Niño modoki. Climate Dynamics, 52, 1383–1394. https://doi.org/10.1007/s00382-018-4196-1
- Wang, X., Guan, C., Huang, R., Tan, W., & Wang, L. (2019b). The roles of tropical and subtropical wind stress anomalies in the El Niño Modoki onset. *Climate Dynamics*, 52(11), 6585–6597. https://doi.org/10.1007/s00382-018-4534-3
- Wang, L., Yu, J.-Y., & Paek, H. (2017). Enhanced biennial variability in the Pacific due to Atlantic capacitor effect. *Nature Communications*, 8, 14887, https://doi.org/10.1038/necommon.14887
- 14887. https://doi.org/10.1038/ncomms14887
 Weisberg, R. H., & Wang, C. (1997). A Western Pacific oscillator paradigm for the El Niño-Southern Oscillation. *Geophysical Research Letters*, 24(7), 779–782. https://doi.org/10.1029/97GL00689
- Wu, Y., & Duan, W. (2012). The amplitude-duration relation of observed El Niño events. Atmospheric and Oceanic Science Letters, 5(5), 367–372. https://doi.org/10.1080/16742834.2012.11447025
- Xie, S.-P., & Philander, S. G. H. (1994). A coupled ocean-atmosphere model of relevance to the ITCZ in the eastern Pacific. Tellus Series A-Dynamic Meteorology and Oceanography, 46(4), 340–350. https://doi.org/10.3402/tellusa.v46i4.15484
- Yu, J.-Y., & Fang, S.-W. (2018). The distinct contributions of the seasonal footprinting and charged-discharged mechanisms to ENSO complexity. Geophysical Research Letters, 45(13), 6611–6618. https://doi.org/10.1029/2018GL077664
- Yu, J.-Y., Lu, M.-M., & Kim, S. T. (2012). A change in the relationship between tropical central Pacific SST variability and the extratropical atmosphere around 1990. Environmental Research Letters, 7(3), 1–6. https://doi.org/10.1088/1748-9326/7/3/034025
- Yun, K.-S., Yeh, S.-W., & Ha, K.-J. (2019). Underlying mechanisms leading to El Niño-to-La Niña transition are unchanged under global warming. Climate Dynamics, 52, 1723–1738. https://doi.org/10.1007/s00382-018-4220-5

CHEN ET AL. 9 of 9